

UC Irvine

UC Irvine Previously Published Works

Title

Sources of air pollution in a region of oil and gas exploration downwind of a large city

Permalink

<https://escholarship.org/uc/item/4s77s4hz>

Authors

Rutter, Andrew P
Griffin, Robert J
Cevik, Basak Karakurt
[et al.](#)

Publication Date

2015-11-01

DOI

10.1016/j.atmosenv.2015.08.073

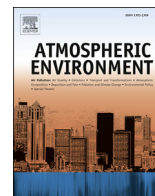
Supplemental Material

<https://escholarship.org/uc/item/4s77s4hz#supplemental>

Copyright Information

This work is made available under the terms of a Creative Commons Attribution License, available at <https://creativecommons.org/licenses/by/4.0/>

Peer reviewed



Sources of air pollution in a region of oil and gas exploration downwind of a large city



Andrew P. Rutter^{a,*}, Robert J. Griffin^a, Basak Karakurt Cevik^a, Kabindra M. Shakya^{a,1}, Longwen Gong^{a,2}, Saewung Kim^{b,3}, James H. Flynn^c, Barry L. Lefer^c

^a Rice University, Civil and Environmental Engineering, Houston, TX 77005, USA

^b National Center for Atmospheric Research, Atmospheric Chemistry Division, Boulder, CO 80305, USA

^c University of Houston, Department of Earth and Atmospheric Sciences, Houston, TX 77204, USA

HIGHLIGHTS

- 6 volatile organic carbon sources are resolved from autoGC and PTR-MS measurements.
- 3 organic aerosol classes are resolved from aerosol mass spectrometer measurements.
- Insights into the organic aerosol sources are gained from VOC sources.
- Reactivities suggest biogenic and oxidized VOCs contribute significantly to ozone.
- Reactivities suggest oil and gas emissions contribute incrementally to local ozone.

ARTICLE INFO

Article history:

Received 3 March 2015

Received in revised form

20 June 2015

Accepted 24 August 2015

Available online xxx

Keywords:

Barnett shale

Hydraulic fracturing

Organic aerosols

PMF

VOCs

Photochemical reactivity

ABSTRACT

The air quality in the outflow from Fort Worth, TX was studied in June 2011 at a location surrounded by oil and gas development in the Barnett Shale. The objectives of this study were to understand the major sources of volatile organic compounds (VOCs) and organic aerosols and explore the potential influence each VOC source had on ozone and secondary organic aerosol formation. Measurements of VOCs were apportioned between six factors using Positive Matrix Factorization (PMF): Natural Gas ($25 \pm 2\%$; $\pm 99\%$ CL); Fugitive Emissions ($15 \pm 2\%$); Internal Combustion Engines ($15 \pm 2\%$); Biogenic Emissions ($7 \pm 1\%$); Industrial Emissions/Oxidation 1 ($8 \pm 1\%$); and Oxidation 2 ($18 \pm 2\%$). Reactivity calculations suggest the Biogenic and Oxidation 2 factors were the most likely VOC sources to influence local ozone. However, enough OH reactivity was calculated for factors related to the oil and gas development that they could incrementally increase O_3 . Three organic aerosol (OA) types were identified with PMF applied to high-resolution time-of-flight aerosol mass spectrometry measurements: hydrocarbon-like OA (HOA; 11% of mass) and two classes of oxidized OA (semi- and less-volatile OOA, SV and LV; 45% and 44%, respectively). The HOA correlated with the Internal Combustion Engine VOC factor indicating that a large fraction of the HOA was emitted by gasoline and diesel motors. The SV-OOA correlated with the oxidized VOC factors during most of the study, whereas a correlation between LV-OOA and the oxidized VOC factors was only observed during part of the study. It is hypothesized that SV-OOA and the oxidized VOC factors correlated reasonably well because these factors likely were separated by at most only a few oxidation generations on the oxidation pathway of organic compounds.

© 2015 Elsevier Ltd. All rights reserved.

* Corresponding author. Current address: S.C. Johnson & Sons Inc., Science and Technology, Racine, WI 53403, USA.

E-mail address: andrew.p.rutter@gmail.com (A.P. Rutter).

¹ Current address: University of Massachusetts, Environmental Health Sciences, Amherst, MA 01003, USA.

² Current address: California Air Resources Board, Sacramento, CA 95812, USA.

³ Current address: Earth System Science, University of California – Irvine, Irvine, CA 92697, USA.

1. Introduction

Air pollution from oil and gas development by hydraulic fracturing (better known as “fracking”) has affected air quality in some regions of the US (Carter and Seinfeld, 2012; Edwards et al., 2013). Development by fracking is being performed near residential areas in several locations in the US, and concerns have been raised over

the impact of these operations on local air quality. Air pollutants emitted include volatile organic compounds (VOCs), nitrogen oxides (NO_x), carbon monoxide (CO), and organic aerosols (OA). Under appropriate atmospheric conditions, the VOCs and NO_x released can contribute to elevated ozone (O₃) concentrations (Edwards et al., 2013) and are likely to impact formation of secondary particulate matter. These species can originate from a variety of sources such as compressor engines, leaking valves on tanks and pipes, compromised pipe seals, well heads, flares, and fracking trucks (Armendariz, 2009).

The measurements described here were made in a region of oil and gas development in the Barnett Shale near Dallas-Fort Worth, TX (DFW). Air quality monitoring by the Texas Commission on Environmental Quality (TCEQ) within this area indicates that the largest O₃ mixing ratios often are observed to the northwest of the metroplex. The DFW metropolitan area (population ~6.5 M) is currently out of compliance with the O₃ National Ambient Air Quality Standard (NAAQS) (USEPA, 2013a). Though the reasons for the exceedances have not been elucidated fully, two hypotheses have been formed. The first is that elevated O₃ concentrations during the summer are caused solely by pollution transported from the urbanized area to the northwest. The second is that emissions associated with the oil and gas development enhance O₃ concentrations above those associated with the urban outflow.

This study explores the potential influence of VOCs emitted from the Barnett Shale development and the DFW metroplex on O₃ and organic aerosols. The VOCs emitted from oil and gas development and urban centers include alkanes, alkenes, and aromatics. While this list is only a subset of atmospheric VOCs, they are the most relevant to this study. Organic aerosols are a complex mixture of carbon-based compounds that are low enough in vapor pressure to exist partially or fully in the condensed phase (Jimenez et al., 2009; Donahue et al., 2011a; Donahue et al., 2011b; Chan et al., 2013). Freshly emitted aerosols, including those from the sources associated with oil and gas operations discussed previously, typically are composed of hydrocarbons, whereas compounds with oxygen and nitrogen heteroatoms are more prevalent in secondary OA (SOA, formed in situ from VOC oxidation products) or primary OA (POA) that has been aged by the atmosphere. In contrast to VOCs, direct emission of POA over land is dominated by human activities (Zhang et al., 2009; Rutter et al., 2014).

To achieve the objectives of this study, the sources of VOCs were inferred using the EPA Positive Matrix Factorization (PMF) model 3.0 which resolves source signatures contributing to environmental measurements (Norris et al., 2008). Next, the reactivities of the identified VOC sources with respect to the hydroxyl radical (OH) were calculated to provide insight into which sources may impact local O₃ formation in the outflow from DFW as it moves across the Barnett Shale. Finally, OA was apportioned into compositional classes using a special version of PMF for apportioning Aerosol Mass Spectrometer (AMS) data (Ulbrich et al., 2009), and the sources of these classes were considered based on the results from the VOC PMF.

2. Methods

2.1. Site description

The Eagle Mountain Lake (EML) site (Fig. S1) was located approximately 30 km northwest of the western edge of the DFW metroplex on flat Texas Air National Guard property (32° 59'16" N, 97° 28' 37" W; +32.987891°, -97.477175°; 226 m above sea level) where a small but significant number of uncounted cattle are allowed to roam. The site is slightly to the west (~3 km) of a minor state highway (two lanes each way) and includes sparse trees and

bushes. The surrounding area is sparsely populated, and EML itself is located just to the west (~2 km) of the site. Two small airports are located close to the site, the first to the east (~10 km) and the second to the west-southwest (~1 km). Numerous natural gas operations are in close proximity to the EML site (Fig. S1). As a result, EML is an appropriate location at which to make close-field measurements of primary emissions from natural gas operations. In addition, due to the prevailing wind (Fig. 1), measurements made at EML captured pollution in the urban outflow from FW after a few hours of advection and processing based on distance and wind speed. Predominant flow from the south-southeast was confirmed by Hybrid Single-Particle Lagrangian Integrated Trajectory modeling (Draxler and Rolph, 2013).

2.2. Measurements

The TCEQ operates a continuous air monitoring station at this location. Of most relevance to the work presented here are VOC data collected using an automated gas chromatograph (auto-GC); these data focus primarily on light hydrocarbons collected on an hourly basis. During June 2011, researchers from several institutions performed air quality measurements at EML to complement these auto-GC measurements. Measurements used in this study include aerosol composition measured with a high-resolution time-of-flight AMS (HR-ToF-AMS, Aerodyne, Billerica, MA), VOCs measured with a proton transfer reaction mass spectrometer (PTR-MS; IONICON Analytik, Innsbruck, Austria), particulate black carbon (BC) with an aethalometer (MicroAeth; AethLabs, San Francisco, CA), water soluble aerosol composition measured with a particle-into-liquid sampler (PILS, Brechtel Manufacturing, Inc., Hayward, CA) connected to two ion chromatographs (Dionex, Sunnyvale, CA), key trace gases (O₃, sulfur dioxide (SO₂), CO, and NO_x; Thermo Fisher Scientific, Sunnyvale, CA), planetary boundary layer heights (PBLH) measured with a ceilometer (Vaisala, Woburn, MA), and standard meteorological parameters (wind speed and direction, temperature, relative humidity, etc.) made with a variety of sensors. More detailed information about data collection is provided in the [Supplemental Information \(SI\)](#).

2.3. Reactivity calculations

Reactivity with respect to OH was calculated for each identified VOC source to probe its potential influence on local O₃ formation. The reactivity (s^{-1}) of an individual VOC i is defined as the product of k_i , the reaction rate coefficient of VOC i with OH at the given temperature ($\text{cm}^3 \text{molec}^{-1} \text{s}^{-1}$), and the concentration of VOC i (molec cm^{-3}). PMF assumes that the relative contributions of individual VOCs to a source factor j (χ_{ij} , from PMF results) are constant across the entire time period. As a result, the reactivity of VOC i from factor j (R_{ij}) can be found from the product of χ_{ij} and R_i . To find the reactivity of a given source (R_j), R_{ij} values are summed over all VOCs.

2.4. Positive matrix factorization

VOCs were apportioned between six sources using EPA PMF 3.0 (Norris et al., 2008). This model seeks co-variance in user-provided time series of concentrations of species (the uncertainties for which also are required) to determine statistically a set of factors that can be recombined to account for as much of the total measured mass as possible. Based on the predominance of species that fall into a given factor, it is possible to attribute that factor to a source. In addition, the user can determine which factor solution (five, six, seven, etc. factors) is most appropriate based on published factor

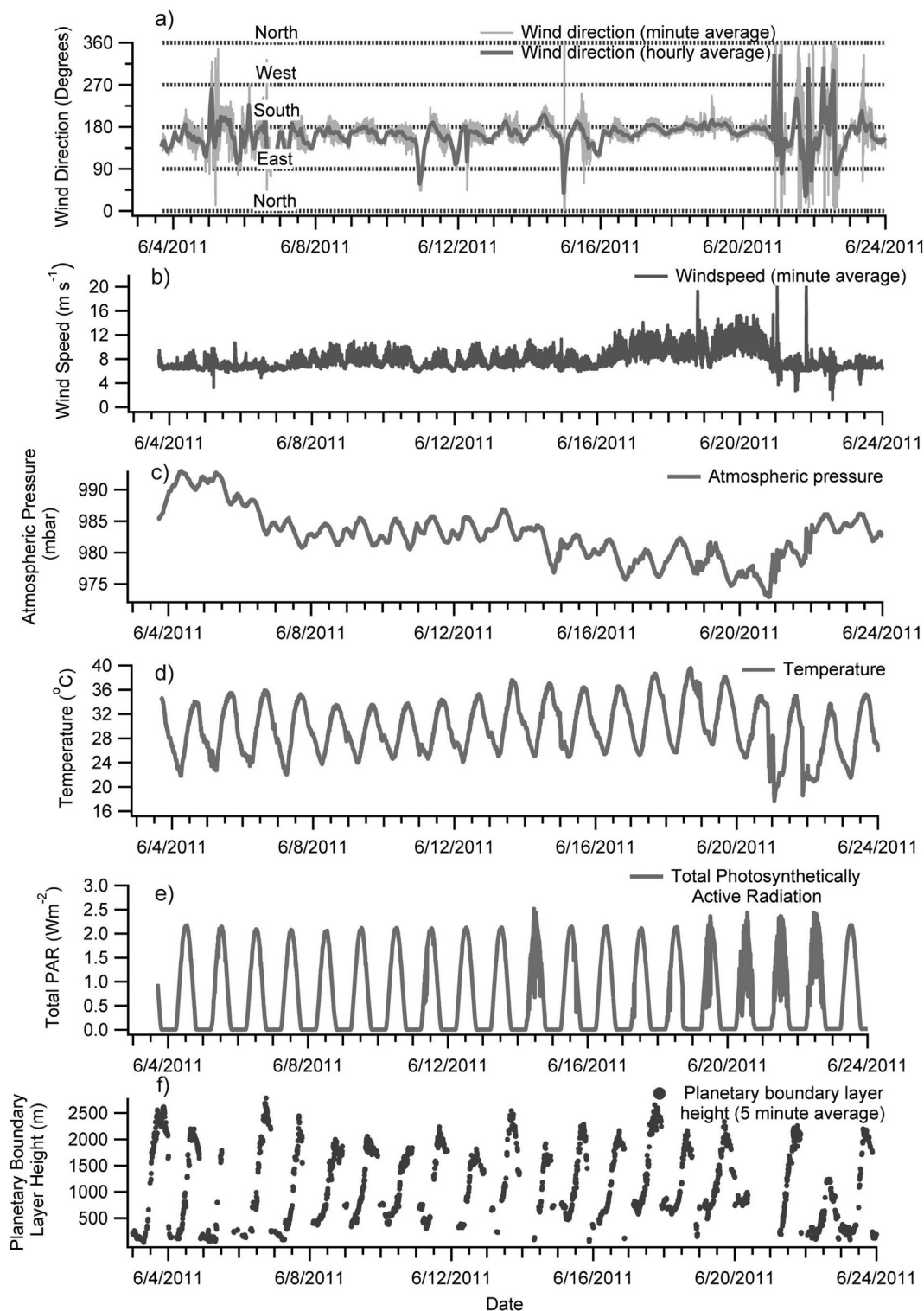


Fig. 1. Time series of meteorological parameters measured at Eagle Mountain Lake (CAMS 75) between 6/3/2011 and 6/23/2011. a.) Wind direction; b.) Wind speed; c.) Pressure; d.) Temperature; e.) Total PAR; f.) Boundary layer height.

compositions, model residuals, ratios of observed to predicted measurements, relationships of known tracers to sources, diurnal profiles, interpretation of structure in the time series, an understanding of the surrounding sources, and the meteorological conditions. A review of the PMF application is provided in the SI.

A separate PMF model was used with the HR-ToF-AMS data

(Ulbrich et al., 2009). In this model representative spectra (assigned to various OA types) are determined as factors. Over the entire time series, the representative spectra that result in the minimization between observed and calculated spectra are determined. These spectra are then assigned to the various types of OA based on comparison to published PMF studies of AMS data and correlations

to time series of other pollutants. Based on the linear combination of these spectral factors to yield the total spectrum, fractions of the total OA concentration are calculated and assigned to each OA type. This methodology results in time series of individual OA components as well as average spectra that describe each OA component.

2.5. Nomenclature

Historically, AMS OA factors resolved by PMF have been described using nomenclature such as hydrocarbon-like OA (HOA), oxidized OA (OOA I and II), low volatility (LV)-OOA, and semi-volatile (SV)-OOA to indicate the relative levels of oxidation or to identify a particular source type (Ulbrich et al., 2009; Zhang et al., 2011). These labels are qualitative and are not ideal for the comparison of factors derived from different studies. This is because the overall oxidation state of OA associated with an air mass is the result of a complex mixture of direct emission, formation of SOA from VOC precursors by various routes, heterogeneous oxidation of condensed-phase material, etc. For this reason, the OA components that are identified by PMF and labeled by an investigator as OOA I and OOA II in one study may not be exactly the same in composition as aerosols given the same designation in a different study or within different time periods within the same study. For this study, the terminology uses HOA, SV-OOA (less oxidized), and LV-OOA (more oxidized) for consistency with previous work.

3. Results and discussion

3.1. Meteorology

Meteorological conditions are summarized in Fig. 1. The campaign was characterized by winds from the direction of DFW (from the southeast) for much of the campaign, with increased variability during meteorological transitions. Wind speeds were between 1 and 21 m s⁻¹ and averaged 8 m s⁻¹. Temperatures ranged between 18 °C and 40 °C, and conditions were sunny. The only precipitation occurred during a heavy thunderstorm on 6/21. The atmospheric pressure ranged between 973 mbar and 993 mbar. The observed pressure and thunderstorm activity show that a front passed over the site on 6/21. Back trajectories indicate that changes in meteorology were consistent with changes in air mass trajectories (Draxler and Rolph, 2013). The PBLH typically varied between 40 m and 1680 m during the early morning hours and between 1500 m and 2500 m in the afternoon, except on 6/22 when the afternoon maximum was 1200 m. Lower PBLHs were observed for long periods overnight from 6/3 until 6/7 and from 6/22 onwards, a characteristic not seen during the rest of the campaign.

3.2. Gas-phase and BC data overview

Overviews of measured CO, BC, SO₂, NO_x, and O₃ are given in Table 1 and Fig. S2. The concentrations of the primary gaseous pollutants (CO, SO₂, and NO_x) were typically low, with short-lived nocturnal increases interpreted as impacts from local point

sources. The values observed were consistent with the rural nature of the measurement site and the presence of point sources upwind (USEPA, 2013b). An increase in NO_x due to lightning was also observed during the thunderstorm (Choi et al., 2005). The BC concentrations were similar to urban measurements (USEPA, 2012) and higher than expected considering the rural nature of EML, indicating the potential impact of sources close to the site. Daily maximum O₃ concentrations were generally higher during periods of high pressure and lower during the middle of the study period leading up to the thunderstorm on 21 June. On three days (6, 22, and 23 June) the 8-h O₃ concentrations exceeded the NAAQS of 75 ppb.

The subset of VOC concentrations presented (Table 2 and Fig. 2) are generally consistent with rural measurements (Guo et al., 2004; Vlasenko et al., 2009). Most VOCs exhibit lower mixing ratios than in urban measurements (Liu et al., 2008; Leuchner and Rappenglück, 2010) and plumes, with the exception of acetone which was similar to measurements made downwind of Mexico City (de Gouw et al., 2009; Bon et al., 2011).

Alkanes typically were highest in concentration during the early morning hours when the PBLH was at a minimum, especially early in the campaign (5–7 June). Back trajectories and wind directions during these periods show the air usually approached the site from an area of well heads and other oil and gas infrastructure (Fig. S1). Aromatics showed similar enhancements during these periods. Other periods that exhibited enhanced aromatic mixing ratios corresponded to wind directions associated with other oil and gas operations (that likely have a different emissions profile) and with the small local airports. A distinct period of elevated biogenic influence (based on isoprene and monoterpenes) was observed during the few days leading up to and including the thunderstorm on 21 June. Back trajectories for 12:00 and 18:00 local time on these days indicate that air masses typically came from the southwest and not directly from DFW. It is assumed that these areas are more densely forested based on on-line satellite images. Concentrations of monoterpenes reached a campaign maximum after the thunderstorm on 6/21, which was nearly twice as large as the next highest concentration (Haase et al., 2011).

3.3. VOC PMF

The results from the EPA PMF 3.0 for the VOC data are shown in Figs. 3 and 4, with statistics presented in Table 3. The profiles for each source type indicate how each species is distributed between different inferred sources (Fig. 3). For example, the ethane percentages across the six factors would add up to 100% if all ethane mass could be attributed.

The Natural Gas factor contained most of the short chain alkanes such as ethane and propane (Buzcu and Fraser, 2006; Brown et al., 2007) and was higher in concentration at night when the PBLH was lower (Fig. 4). This was consistent with emissions from oil and gas development infrastructure surrounding the monitoring site. A factor containing most of the C₄ through C₇ alkanes was thought to be fugitive emissions of gasoline from fuel stations and/or product

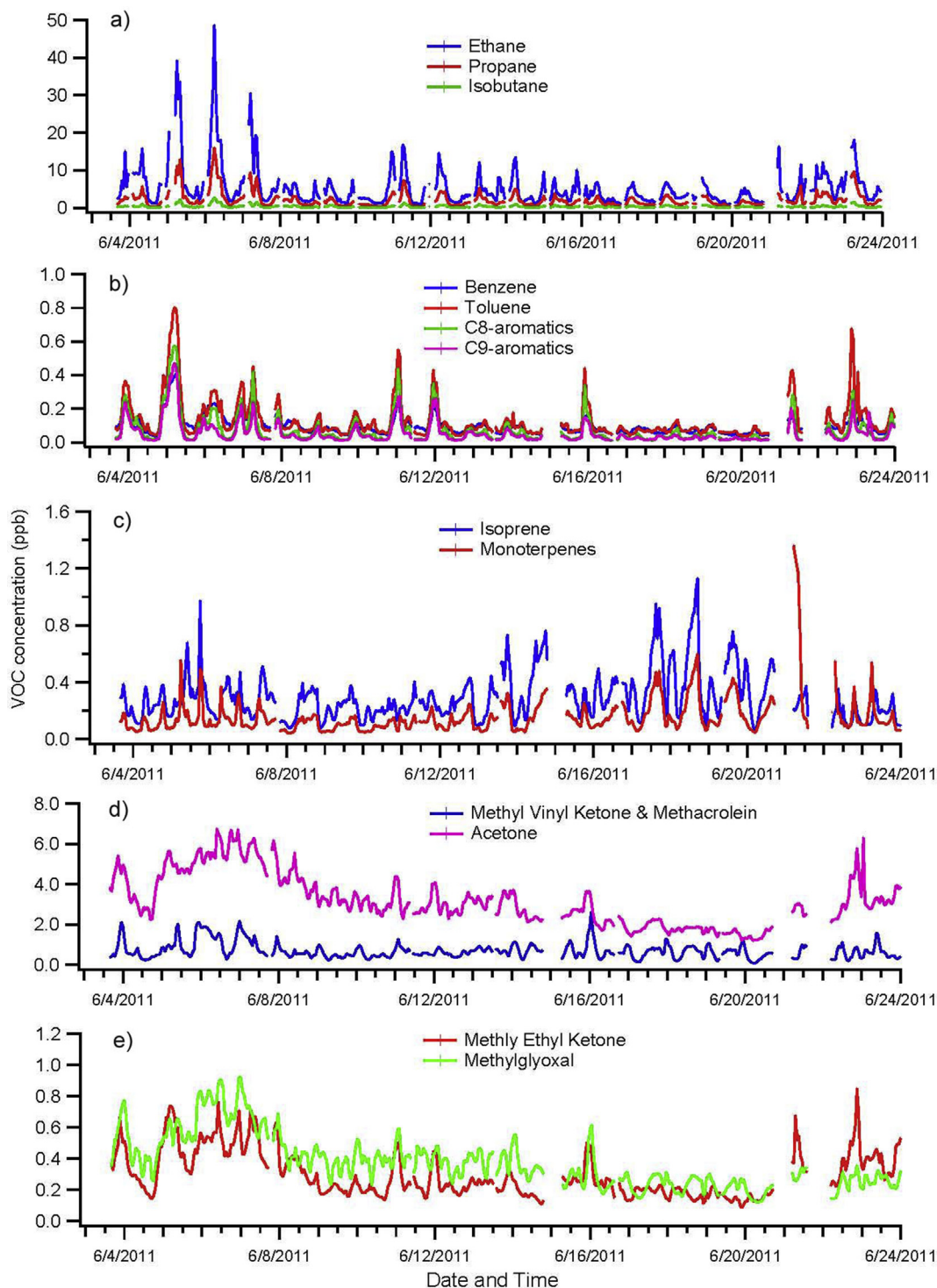
Table 1
Statistics for hourly averages of measured CO, BC, SO₂, NO_x, O₃, and OA. Min represents the minimum observed value, and max represents the maximum observed value. 95th indicates the 95th percentile value.

Statistics	Carbon monoxide (ppm)	Black carbon (µg m ⁻³)	Sulfur dioxide (ppb)	NO _x (ppb)	Ozone (ppb)	Organic aerosols (µg m ⁻³)
Mean	0.15	0.5	0.4	3.7	40.8	4.6
Median	0.13	0.4	0.2	2.1	39.7	3.7
Min	0.05	0.1	BDL	0.2	5.05	0.7
Max	0.86	1.9	4.9	30.6	106.1	16.7
95th	0.24	1.2	1.1	11.4	74.3	9.2

Table 2

Statistics defined in Table 1 for key VOCs measured with an autoGC and a PTR-MS calculated using hourly averages. Units are ppb.

Statistics	Ethane	Propane	Toluene	Benzene	C ₈ aromatics	C ₉ aromatics	Isoprene	Mono-terpenes	Acetone	MVK & methacrolein	Methyl ethyl ketone	Methyl glyoxal
Mean	5.5	2.2	0.13	0.10	0.07	0.05	0.29	0.15	3.2	0.70	0.30	0.38
Median	3.6	1.5	0.09	0.08	0.04	0.03	0.25	0.12	3.0	0.61	0.24	0.34
Min	0.8	0.2	0.04	0.03	0.01	0.01	0.06	0.04	1.2	0.09	0.09	0.12
Max	48.7	16.0	0.80	0.43	0.57	0.47	1.13	1.36	6.7	2.61	0.85	0.92
95th	17.7	7.4	0.35	0.22	0.25	0.18	0.64	0.37	5.7	1.57	0.59	0.75

**Fig. 2.** Time series of VOC concentrations during the campaign. a.) Light alkanes; b.) Aromatics; c.) Biogenic VOCs; d.) Oxygenated VOCs; e.) Additional oxygenated VOCs.

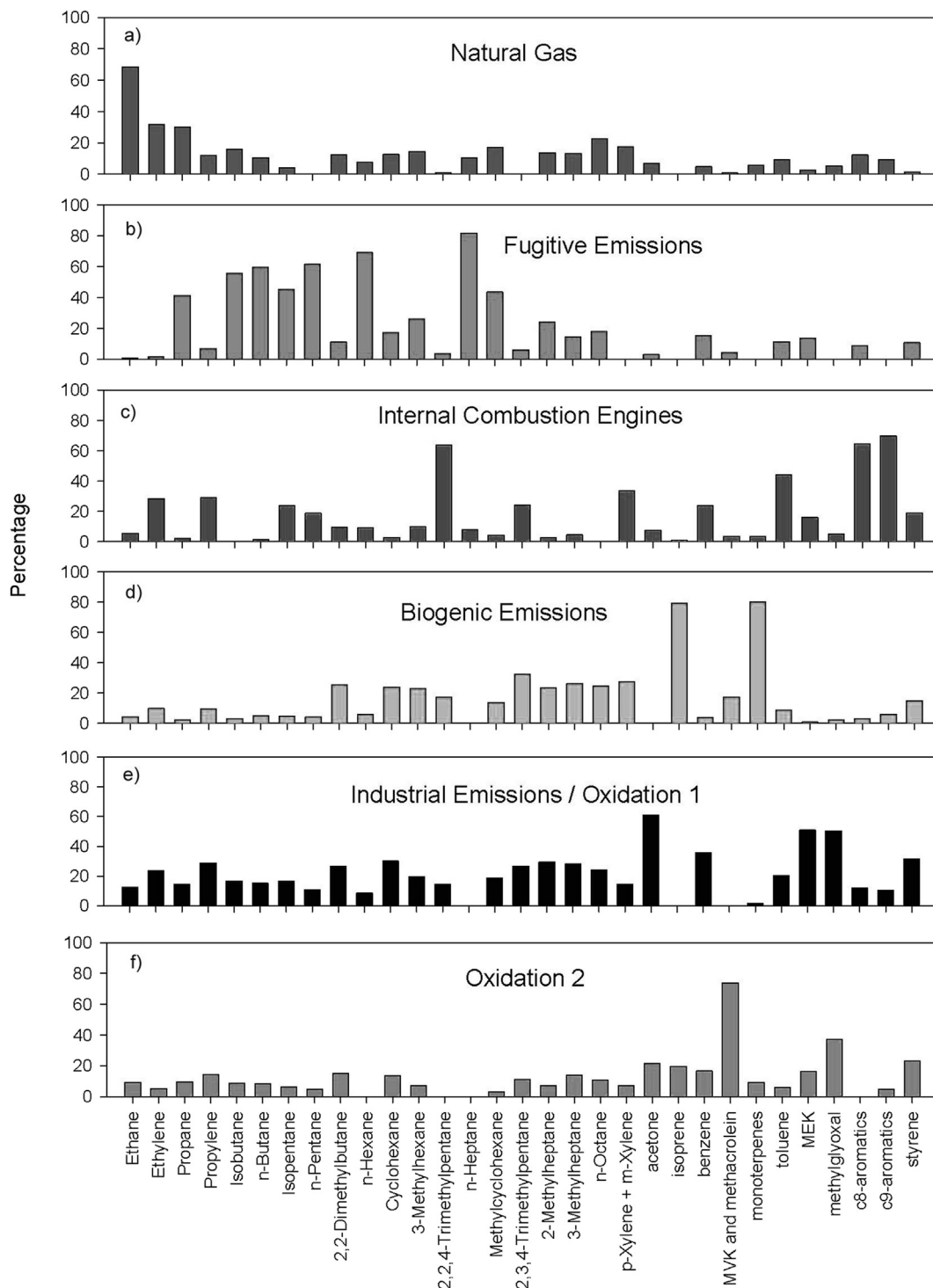


Fig. 3. PMF profiles for VOCs during the campaign. a.) Natural Gas; b.) Fugitive Emissions; c.) Internal Combustion Engines; d.) Biogenic Emissions; e.) Industrial Emissions/Oxidation 1; f.) Oxidation 2.

from oil and gas development infrastructure (Fujita et al., 1994; Buzcu and Fraser, 2006; Brown et al., 2007; USEPA, 2014). Furthermore, the concentration of this Fugitive Emissions factor was higher overnight when the PBLH was lower, consistent with local, continuously emitting sources. The Fugitive Emissions time series is highly correlated with the Natural Gas factor (Fig. S3).

The assignment of the Internal Combustion Engine factor was based on apportionment of aromatics and 2,2,4-trimethylpentane,

which are important components of gasoline (USEPA, 2000). This factor peaked both overnight (boundary layer) and at times shifted slightly from traditional rush hour periods (related to transport time from DFW).

The Biogenic factor contained most of the isoprene and monoterpenes (Fig. 3). As a result, the Biogenic factor shows characteristics that correspond to the isoprene and monoterpene time series (Figs. 2 and 4). The diurnal profile of the Biogenic factor is

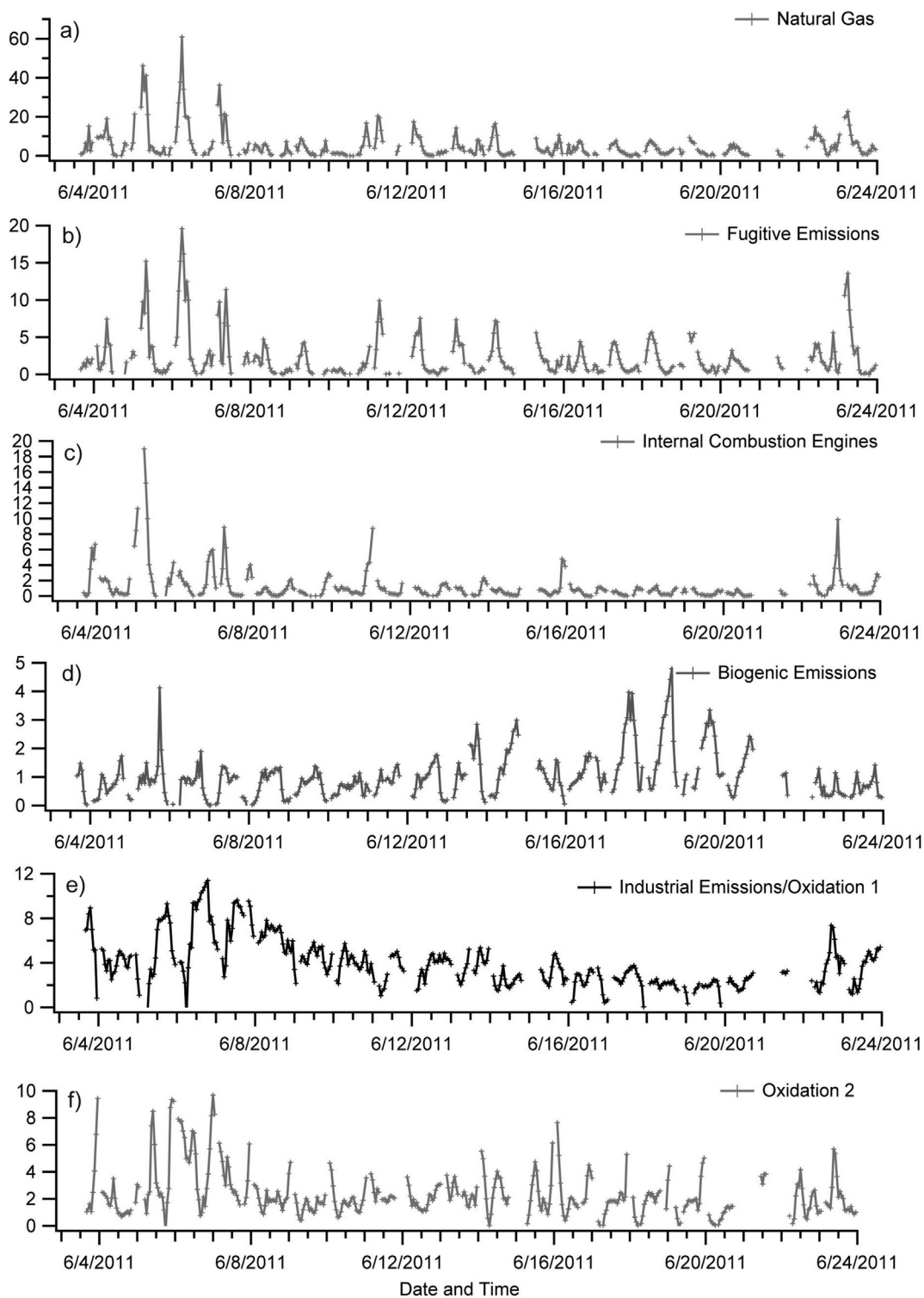


Fig. 4. Time series of PMF factors for VOCs during the campaign. a.) Natural Gas; b.) Fugitive Emissions; c.) Internal Combustion Engines; d.) Biogenic Emissions; e.) Industrial Emissions/Oxidation 1; f.) Oxidation 2. Y-axis units are ppb.

consistent with plant emissions related to photosynthesis and affected by temperature (Fig. 1 and Fig. S4). A small fraction of the longer chain alkanes and aromatics measured by the auto-GC are allocated to this factor. This may be because biogenic compounds are always present in polluted air or due to biogenic emissions of non-terpenoid compounds (White et al., 2009).

The Industrial Emissions/Oxidation 1 factor represents a combination of primary industrial VOCs mixed with oxidized VOCs. This factor included significant loadings of acetone, methyl ethyl ketone (MEK), methylglyoxal, benzene, styrene and several of the alkanes and alkenes. A weak diurnal variation is seen in the Industrial Emissions/Oxidation 1 factor, with lowest concentrations during

Table 3
Statistics defined in Table 1 for the VOC and OA factors calculated using hourly averages.

Statistics	VOC factors (ppb)						OA factors ($\mu\text{g m}^{-3}$)		
	Natural Gas	Fugitive emissions	Internal combustion engines	Biogenic	Industrial emissions/oxidation 1	Oxidation 2	HOA	SV-OOA	LV-OOA
Mean	5.4	2.3	1.2	1.0	3.8	2.4	0.5	2.5	1.7
Median	2.5	1.1	0.7	0.8	3.3	2.0	0.3	1.6	1.4
Min	0.0	0.0	0.0	0.0	0.0	0.0	0.0	0.0	0.0
Max	61.0	19.6	19.0	4.8	11.4	9.7	3.2	9.8	4.6
95th	21.1	9.9	4.3	2.6	8.8	6.1	1.4	6.8	3.7

local morning hours. Acetone and MEK both have primary and secondary sources (de Gouw et al., 2005; Vlasenko et al., 2009), while methyl glyoxal is an oxidation product of both anthropogenic and biogenic VOCs (Nishino et al., 2010; Galloway et al., 2011; Henry et al., 2011). The trend is consistent with emissions from DFW that are being oxidized during transport to the site.

The Oxidation 2 factor was found to have significant loadings of the isoprene-oxidation products methyl vinyl ketone (MVK), methacrolein (MACR), and methylglyoxal (Pierotti et al., 1990; Galloway et al., 2011). Because of the short lifetimes of isoprene under highly-photochemically active scenarios, it is believed that Oxidation 2 represents rapid oxidative processing of local biogenic emissions. The diurnal trend is bimodal in nature, exhibiting a smaller daytime mode which peaks around midday consistent with a secondary formation process, and a larger nighttime mode caused by PBLH dynamics (Fig. S4) (Montzka et al., 1993).

3.4. Reactivity calculations

The relative potential impacts of VOC sources on O_3 formation was explored by calculating the combined OH reactivity of each source profile using the methodology described previously (Fig. 5). The biogenic factor contributed the most OH reactivity (42%). Oxidation 2, thought to be related to biogenic oxidation, was the next largest contributor (28%). These two factors indicate the predominance of biogenic activity with regard to potential local O_3 formation (on average, 70%). The next most important factor was that for Industrial Emissions/Oxidation 1 (10%), which is related to outflow from DFW. In contrast, Internal Combustion Engine emissions originated from both DFW and the oil and gas development, contributed an average of 7% of the OH reactivity. Natural Gas and Fugitive Emissions are thought to be related predominantly to oil and gas operations. Together, they contributed the final 13% of the average OH reactivity. Although a smaller percentage of the total OH reactivity, they might incrementally increase O_3 concentrations within the DFW monitoring domain. The relative contributions between sources varied diurnally but were generally consistent throughout the course of the 3 week study period (Fig. 5).

3.5. HR-ToF-AMS PMF

The PMF model applied to the HR-ToF-AMS OA measurements best resolved three factors robustly (Fig. 6 and Fig. S5; Table 3). Factor 1 is attributed to HOA due to the large contribution of C_xH_y fragments even at large m/z and only a modest contribution from CO_2^+ ($m/z = 44$). Factors 2 and 3 have much more significant contributions from CO_2^+ and much less significant contributions from the various C_xH_y fragments. At first glance there appears to be little difference between these two OOA factors, although closer inspection reveals that the SV-OOA has a smaller signal ratio for m/z 44 to m/z 43 (C_3H_7^+) and larger contributions from fragments at larger m/z values compared to the LV-OOA.

Time series and diurnal profiles of the OA factors show both

similarities and differences to the VOC factors (Fig. 6 and Fig. S6). The HOA time series show characteristics very similar to those of the Internal Combustion Engine factor (Fig. 4 and Fig. S6). A regression of the HOA and Internal Combustion Engine factors reveals a modest correlation (Fig. 7, top panel), which is supported by a positive correlation between HOA and CO (Fig. S7, top panel). These correlations indicate that HOA is in part due to mobile sources, likely due to emission of lubricating oil rather than unburned fuel (Schauer et al., 1999). Stationary engines are used to drive compressors in the oil and gas distribution lines on the Barnett Shale (Armendariz, 2009). No correlation was observed between HOA and other primary VOCs such as those that would be emitted from these engines, indicating the probable lack of significant OA emissions associated with these VOC emission processes.

The SV-OOA time series shows increased concentrations at the start and end of the study (Fig. 6), consistent with elevated nocturnal precursor VOCs (such as the aromatics shown in Fig. 2b), oxidized VOCs, and HOA during these periods (Figs. 2 and 6). However, the concentrations of SV-OOA decrease after 22:00 (Fig. S6). This behavior is also apparent in acetone, MEK, methyl glyoxal and BC (Fig. 2), implying that SV-OOA is not being generated locally at night at a rate in excess of its loss rate. The trends in the median concentrations in the diurnal profile of SV-OOA are consistent with the daytime formation of an oxidized species upwind that is then delayed by a few hours in arriving at the site. Similarities in the features of the SV-OOA and oxidized VOCs time series also suggests that these species may be chemically related during these periods of the study.

Elevated concentrations of SV-OOA are observed during the middle of the study, a trend which is not reflected in the gaseous or BC measurements except isoprene. It is possible the SV-OOA during this period is driven more strongly by oxidation of this biogenic VOC. The trend also is observed in LV-OOA. Similarities between the OOA factor trends, although vague in some instances, are observed in the latter part of the campaign (12–24 June). This suggests that the OOA factors may be chemically related during the second half of the study, but not the first. The diurnal profile of LV-OOA shows increased concentrations towards the late afternoon and evening hours, similar to SV-OOA (Fig. S6). This trend is consistent with formation of LV-OOA, potentially from aging of SV-OOA during transport from further upwind.

The SV-OOA factor was correlated with the sum of the Industrial Emissions/Oxidation 1 and Oxidation 2 VOC factors despite the mixed biogenic/industrial influence on the oxidation signals (Fig. S7, bottom panel), particularly after measurements following the meteorological transition on 6/21 were excluded (Fig. 7, bottom panel). It is possible that SV-OOA and the oxidized VOC factors correlated reasonably well because these factors may be separated by only a few steps if considering multi-generational oxidation processes (Jimenez et al., 2009). That is, the VOC Oxidation factors include first- or second-generation oxidation products such as acetone, MVK, MACR, etc. The presence of first and second generation oxidation products in the VOC oxidation factors suggests they

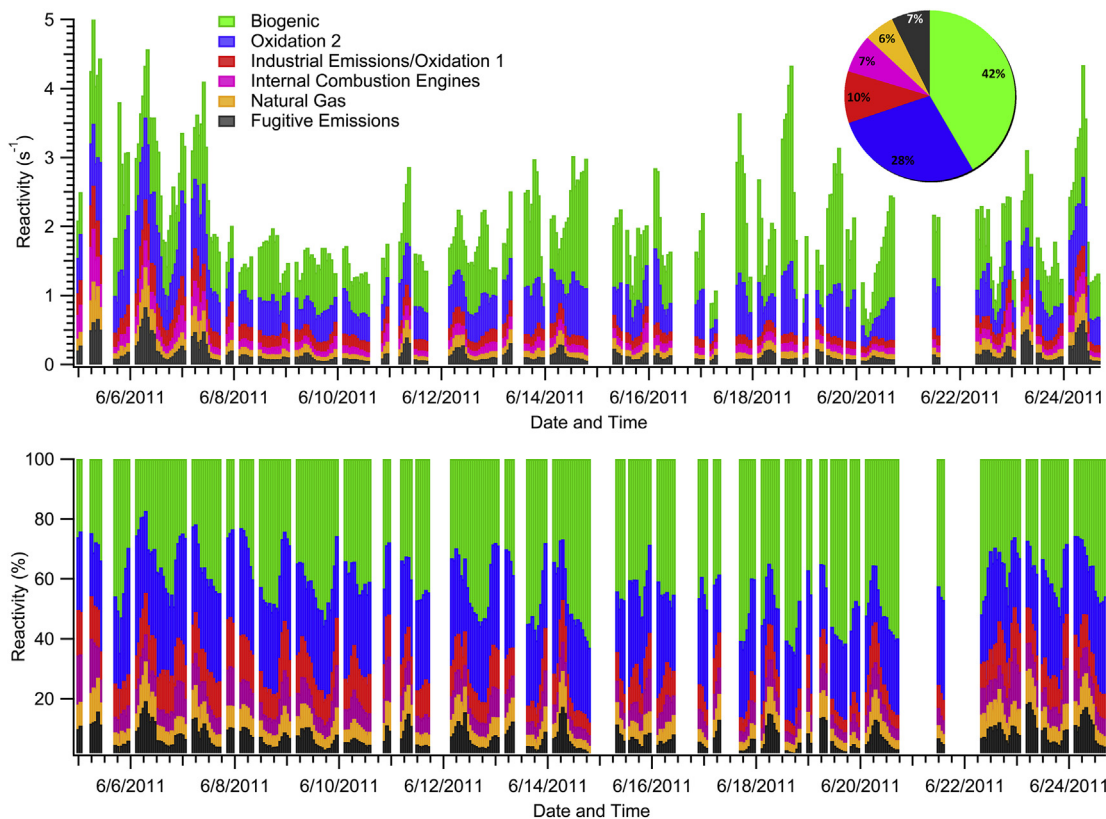


Fig. 5. Reactivity attributed to specific VOC factors during the campaign expressed in absolute values (top panel) and relative fractions (bottom panel); the inset pie chart shows the average contribution of each factor across the campaign.

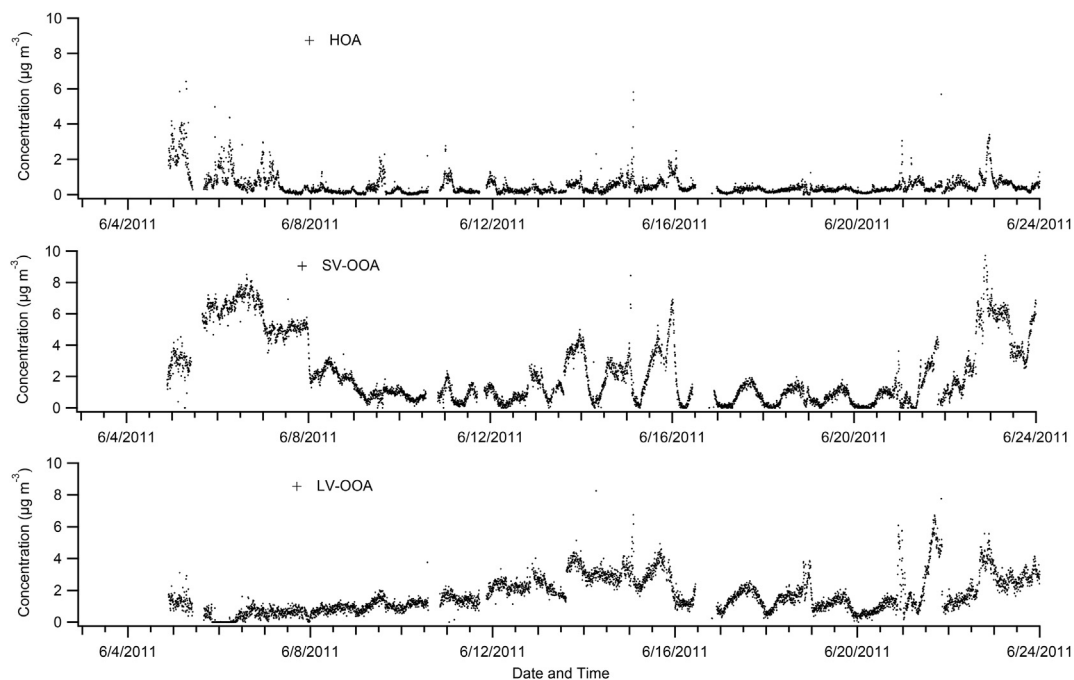


Fig. 6. PMF time series for OA types. Measurements are presented as 5 min averages. Top = HOA; middle = SV-OOA; bottom = LV-OOA.

were formed or emitted in the DFW area. The correlation between SV-OOA and the VOC oxidation factors suggests that much of this component was formed locally during the day.

Correlation between the LV-OOA and the oxidized VOC factors

(Fig. 8) revealed two distinct relationships, with the shift between the two occurring on 6/9 due to a meteorological transition (Fig. 1; see wind direction, wind speed, barometric pressure). The division between the data sets occurs within a few days of the change in

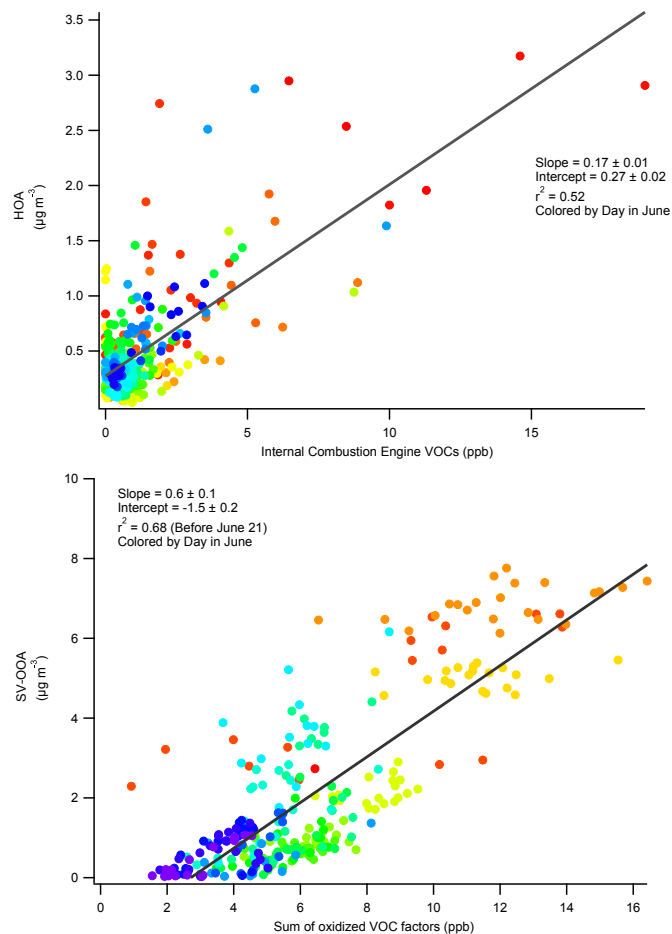


Fig. 7. Regressions between HOA and VOC from Internal Combustion Engines (top panel) and between SV-OOA and the sum of oxidized VOC factors with data for certain dates excluded as discussed in the text (bottom panel).

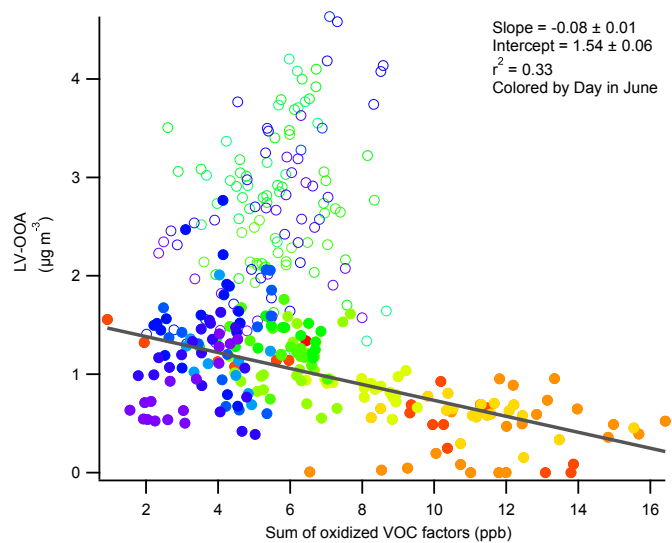


Fig. 8. Regression between LV-OOA and the sum of oxidized VOC factors. The panel includes all data in the study but only the filled circles are fitted. Open circles are measurements made before meteorological transitions on 6/9 and after 6/21. Data markers are colored by day in June.

relationship observed between SV-OOA and LV-OOA in Fig. 6. Little or no correlation is observed between LV-OOA and the oxidized VOCs at the start of the campaign (open circles). Measurements of LV-OOA after 6/9 and before 6/21 demonstrate a modest inverse correlation with the oxidized VOC factors. This relationship is reasonable for more aged OA. They are further removed from the parent VOCs and the measured oxidized VOCs along the oxidation pathway of organic compounds. The inverse nature of the relationship may imply gas-particle partitioning of oxidized VOCs to form OOA.

4. Conclusions

The objective of this study was to gain insight into the relative influences on air quality of VOC sources in the oil and gas development on the Barnett Shale and in the greater DFW metropolplex. The VOC apportionment of autoGC and PTR-MS measurements revealed six factors and seven sources of VOCs (five primary and two secondary), with one of the factors being a mixture of a primary and secondary sources. Reactivity calculations showed that the majority of OH reactivity was contributed by biogenic sources and oxidized biogenic VOCs. However, enough OH reactivity was calculated for factors related to the oil and gas development that they could incrementally increase O_3 . The OA mass was apportioned into HOA, SV-OOA, and LV-OOA. The HOA showed modest correlations with VOCs associated with internal combustion engines and CO, suggesting that about half of the observed HOA came from this source. The SV-OOA correlated well with the oxidized VOCs until a transition in meteorology occurred towards the end of the study, suggesting that much of SV-OOA originated from oxidized VOCs in the local urban outflow. The LV-OOA exhibited an inverse correlation with the oxidized VOCs for part of the study but did not correlate well outside of this period, suggesting in general that LV-OOA represents a well-aged aerosol. Relationships suggested that most of the OA mass originated from sources unrelated to oil and gas development.

Acknowledgments

Funding was provided by the Texas Commission for Environmental Quality Air Quality Research Program and the Camille and Henry Dreyfus Foundation. Susan Simonet (TCEQ) provided, and assisted with preparing, the VOC data measured by the TCEQ auto GC at EML. Melanie Calzada and Caroline Gutierrez assisted with field activities.

Appendix A. Supplementary data

Supplementary data related to this article can be found at <http://dx.doi.org/10.1016/j.atmosenv.2015.08.073>.

References

- Armendariz, A., 2009. Report: Emissions from Natural Gas Production in the Barnett Shale Area and Opportunities for Cost-effective Improvements. Published by Southern Methodist University.
- Bon, D., Ulbrich, I., de Gouw, J., Warneke, C., Kuster, W., Alexander, M., Baker, A., Beyersdorf, A., Blake, D., Fall, R., 2011. Measurements of volatile organic compounds at a suburban ground site (T1) in Mexico City during the MILAGRO 2006 campaign: measurement comparison, emission ratios, and source attribution. *Atmos. Chem. Phys.* 11, 2399–2421.
- Brown, S.G., Frankel, A., Hafner, H.R., 2007. Source apportionment of VOCs in the Los Angeles area using positive matrix factorization. *Atmos. Environ.* 41, 227–237.
- Buzcu, B., Fraser, M.P., 2006. Source identification and apportionment of volatile organic compounds in Houston, TX. *Atmos. Environ.* 40, 2385–2400.
- Carter, W.P.L., Seinfeld, J.H., 2012. Winter ozone formation and VOC incremental reactivities in the Upper Green River Basin of Wyoming. *Atmos. Environ.* 50, 255–266.

- Chan, A.W.H., Isaacman, G., Wilson, K.R., Worton, D.R., Ruehl, C.R., Nah, T., Gentner, D.R., Dallmann, T.R., Kirchstetter, T.W., Harley, R.A., Gilman, J.B., Kuster, W.C., de Gouw, J.A., Offenberg, J.H., Kleindienst, T.E., Lin, Y.H., Rubitschun, C.L., Surratt, J.D., Hayes, P.L., Jimenez, J.L., Goldstein, A.H., 2013. Detailed chemical characterization of unresolved complex mixtures in atmospheric organics: Insights into emission sources, atmospheric processing, and secondary organic aerosol formation. *J. Geophys. Res. Atmos.* 118, 6783–6796.
- Choi, Y., Wang, Y., Zeng, T., Martin, R.V., Kurosu, T.P., Chance, K., 2005. Evidence of lightning NO_x and convective transport of pollutants in satellite observations over North America. *Geophys. Res. Lett.* 32, L02805.
- de Gouw, J.A., Middlebrook, A.M., Warneke, C., Goldan, P.D., Kuster, W.C., Roberts, J.M., Fehsenfeld, F.C., Worsnop, D.R., Canagaratna, M.R., Pszenny, A.A.P., Keene, W.C., Marchewka, M., Bertman, S.B., Bates, T.S., 2005. Budget of organic carbon in a polluted atmosphere: results from the New England air quality study in 2002. *J. Geophys. Res. Atmos.* 110, D16305.
- de Gouw, J.A., Welsh-Bon, D., Warneke, C., Kuster, W., Alexander, L., Baker, A.K., Beyersdorf, A.J., Blake, D., Canagaratna, M., Celada, A., 2009. Emission and chemistry of organic carbon in the gas and aerosol phase at a sub-urban site near Mexico City in March 2006 during the MILAGRO study. *Atmos. Chem. Phys.* 9, 3425–3442.
- Donahue, N.M., Epstein, S.A., Pandis, S.N., Robinson, A.L., 2011a. A two-dimensional volatility basis set: 1. organic-aerosol mixing thermodynamics. *Atmos. Chem. Phys.* 11, 3303–3318.
- Donahue, N.M., Kroll, J.H., Pandis, S.N., Robinson, A.L., 2011b. A two-dimensional volatility basis set – Part 2: diagnostics of organic-aerosol evolution. *Atmos. Chem. Phys. Discuss.* 11, 24883–24931.
- Draxler, R.R., Rolph, G.D., 2013. HYSPLIT (HYbrid Single-particle Lagrangian Integrated Trajectory) Model NOAA Air Resources Laboratory, College Park, MD.
- Edwards, P.M., Young, C.J., Aikin, K., deGouw, J., Dubé, W.P., Geiger, F., Gilman, J., Helmig, D., Holloway, J.S., Kercher, J., Lerner, B., Martin, R., McLaren, R., Parrish, D.D., Peischl, J., Roberts, J.M., Ryerson, T.B., Thornton, J., Warneke, C., Williams, E.J., Brown, S.S., 2013. Ozone photochemistry in an oil and natural gas extraction region during winter: simulations of a snow-free season in the Uintah Basin, Utah. *Atmos. Chem. Phys.* 13, 8955–8971.
- Fujita, E.M., Watson, J.G., Chow, J.C., Lu, Z., 1994. Validation of the chemical mass balance receptor model applied to hydrocarbon source apportionment in the Southern California air quality study. *Environ. Sci. Technol.* 28, 1633–1649.
- Galloway, M., Huisman, A., Yee, L., Chan, A., Loza, C., Seinfeld, J., Keutsch, F., 2011. Yields of oxidized volatile organic compounds during the OH radical initiated oxidation of isoprene, methyl vinyl ketone, and methacrolein under high-NO_x conditions. *Atmos. Chem. Phys.* 11, 10779–10790.
- Guo, H., Wang, T., Simpson, I.J., Blake, D.R., Yu, X.M., Kwok, Y.H., Li, Y.S., 2004. Source contributions to ambient VOCs and CO at a rural site in eastern China. *Atmos. Environ.* 38, 4551–4560.
- Haase, K.B., Jordan, C., Mentis, E., Cottrell, L., Mayne, H.R., Talbot, R., Sive, B.C., 2011. Changes in monoterpene mixing ratios during summer storms in rural New Hampshire (USA). *Atmos. Chem. Phys.* 11, 11465–11476.
- Henry, S., Kammrath, A., Keutsch, F., 2011. Quantification of gas-phase glyoxal and methylglyoxal via the laser-induced phosphorescence of (methyl) GlyOxal spectrometry (LIPGLOS) method. *Atmos. Meas. Tech. Discuss.* 4, 6159–6183.
- Jimenez, J.L., Canagaratna, M.R., Donahue, N.M., Prevot, A.S.H., Zhang, Q., Kroll, J.H., DeCarlo, P.F., Allan, J.D., Coe, H., Ng, N.L., Aiken, A.C., Docherty, K.S., Ulbrich, I.M., Grieshop, A.P., Robinson, A.L., Duplissy, J., Smith, J.D., Wilson, K.R., Lanz, V.A., Hueglin, C., Sun, Y.L., Tian, J., Laaksonen, A., Raatikainen, T., Rautiainen, J., Vaattovaara, P., Ehn, M., Kulmala, M., Tomlinson, J.M., Collins, D.R., Cubison, M.J., Dunlea, E.J., Huffman, J.A., Onasch, T.B., Alfarra, M.R., Williams, P.I., Bower, K., Kondo, Y., Schneider, J., Drewnick, F., Borrmann, S., Weimer, S., Demerjian, K., Salcedo, D., Cottrell, L., Griffin, R., Takami, A., Miyoshi, T., Hatakeyama, S., Shimono, A., Sun, J.Y., Zhang, Y.M., Dzepina, K., Kimmel, J.R., Sueper, D., Jayne, J.T., Herndon, S.C., Trimborn, A.M., Williams, L.R., Wood, E.C., Middlebrook, A.M., Kolb, C.E., Baltensperger, U., Worsnop, D.R., 2009. Evolution of organic aerosols in the atmosphere. *Science* 326, 1525–1529.
- Leuchner, M., Rappenglück, B., 2010. VOC source–receptor relationships in Houston during TexAQ5-II. *Atmos. Environ.* 44, 4056–4067.
- Liu, Y., Shao, M., Kuster, W.C., Goldan, P.D., Li, X., Lu, S., Gouw, J.A., 2008. Source identification of reactive hydrocarbons and oxygenated VOCs in the summertime in Beijing. *Environ. Sci. Technol.* 43, 75–81.
- Montzka, S.A., Trainer, M., Goldan, P.D., Kuster, W.C., Fehsenfeld, F.C., 1993. Isoprene and its oxidation products, methyl vinyl ketone and methacrolein, in the rural troposphere. *J. Geophys. Res. Atmos.* 98, 1101–1111.
- Nishino, N., Arey, J., Atkinson, R., 2010. Formation yields of glyoxal and methylglyoxal from the gas-phase OH radical-initiated reactions of toluene, xylenes, and trimethylbenzenes as a function of NO₂ concentration. *J. Phys. Chem. A* 114, 10140–10147.
- Norris, G., Vedantham, R., Wade, K., Brown, S., Prouty, J., Foley, C., 2008. EPA Positive Matrix Factorization (PMF) 3.0 Fundamentals & User Guide. US Environmental Protection Agency, Office of Research and Development, Washington, DC.
- Pierotti, D., Wofsy, S.C., Jacob, D., Rasmussen, R.A., 1990. Isoprene and its oxidation products: methacrolein and methyl vinyl ketone. *J. Geophys. Res. Atmos.* 95, 1871–1881.
- Rutter, A.P., Snyder, D.C., Stone, E.A., Shelton, B., DeMinter, J., Schauer, J.J., 2014. Preliminary assessment of the anthropogenic and biogenic contributions to secondary organic aerosols at two industrial cities in the upper Midwest. *Atmos. Environ.* 84, 307–313.
- Schauer, J.J., Kleeman, M.J., Cass, G.R., Simoneit, B.R.T., 1999. Measurement of emissions from air pollution sources. 1. C₁ through C₃₀ organic compounds from medium duty diesel trucks. *Environ. Sci. Technol.* 33, 1578–1587.
- Ulbrich, I.M., Canagaratna, M.R., Zhang, Q., Worsnop, D.R., Jimenez, J.L., 2009. Interpretation of organic components from positive matrix factorization of aerosol mass spectrometric data. *Atmos. Chem. Phys.* 9, 2891–2918.
- USEPA, 2000. 2,2,4-Trimethylpentane.
- USEPA, 2012. Report to Congress on Black Carbon.
- USEPA, 2013a. The Green Book Nonattainment Areas for Criteria Pollutants.
- USEPA, 2013b. Report on the Environment.
- USEPA, 2014. SPECIATE Database.
- Vlasenko, A., Slowik, J.G., Bottenheim, J.W., Brickell, P.C., Chang, R.Y.W., Macdonald, A.M., Shantz, N.C., Sjostedt, S.J., Wiebe, H.A., Leitch, W.R., Abbatt, J.P.D., 2009. Measurements of VOCs by proton transfer reaction mass spectrometry at a rural Ontario site: sources and correlation to aerosol composition. *J. Geophys. Res. Atmos.* 114, D21305.
- White, M.L., Russo, R.S., Zhou, Y., Ambrose, J.L., Haase, K., Frinak, E.K., Varner, R.K., Wingenter, O.W., Mao, H., Talbot, R., Sive, B.C., 2009. Are biogenic emissions a significant source of summertime atmospheric toluene in the rural North-eastern United States? *Atmos. Chem. Phys.* 9, 81–92.
- Zhang, Q., Jimenez, J., Canagaratna, M., Ulbrich, I., Ng, N., Worsnop, D., Sun, Y., 2011. Understanding atmospheric organic aerosols via factor analysis of aerosol mass spectrometry: a review. *Anal. Bioanal. Chem.* 401, 3045–3067.
- Zhang, Y., Sheesley, R.J., Schauer, J.J., Lewandowski, M., Jaoui, M., Offenberg, J.H., Kleindienst, T.E., Edney, E.O., 2009. Source apportionment of primary and secondary organic aerosols using positive matrix factorization (PMF) of molecular markers. *Atmos. Environ.* 43, 5567–5574.